

## Interaction of massless Dirac electrons with acoustic phonons in graphene at low temperatures

S. S. Kubakaddi

*Department of Physics, Karnatak University, Dharwad-580 003, Karnataka, India*

(Received 22 August 2008; revised manuscript received 23 October 2008; published 9 February 2009)

Interaction of massless electrons with the acoustic phonons is studied in two-dimensional (2D) graphene at low temperatures by calculating phonon drag thermopower  $S^g$  and hot-electron energy-loss rate  $F(T)$ .  $S^g$  and  $F(T)$  are studied as a function of temperature  $T$  and electron concentration  $n_s$ . For very low temperatures  $S^g \sim T^3$  and  $F(T) \sim T^4$  in contrast to  $S^g \sim T^4$  and  $F(T) \sim T^5$  of unscreened deformation-potential coupling in usual 2D systems. We find that  $S^g$  is related to the phonon limited mobility  $\mu_p$  by  $S^g \mu_p = v_s \Lambda T^{-1}$  ( $v_s$  is the phonon velocity and  $\Lambda$  is the phonon mean-free path) validating Herring's law for linear dispersion of electrons in graphene. In the low-temperature limit  $S^g, F(T) \sim n_s^{-1/2}$ . For comparison diffusion thermopower  $S^d$  is calculated and  $S^d \sim T, n_s^{-1/2}$ . Our results are compared with those in the usual 2D systems.

DOI: 10.1103/PhysRevB.79.075417

PACS number(s): 72.10.Di, 72.20.Ht, 72.20.Pa, 73.50.Lw

## I. INTRODUCTION

Since the recent discovery of the quantum Hall effect in two-dimensional (2D) graphene which exhibits remarkably high electronic quality with the mobility  $\mu$  as high as  $2 \times 10^4$  cm<sup>2</sup>/V s, there has been a great deal of interest in its electronic properties both theoretically and experimentally.<sup>1-3</sup> It is a very important development in the low-dimensional electronic phenomenon in nanostructures, as the 2D graphene systems show the potential to become high-speed and high power transistors, and revolutionize the gas sensors capable of detecting individual molecules. This could lead to enormous changes in nanoelectronics of the future. Investigations of Novoselov *et al.*<sup>2</sup> and Zhang *et al.*<sup>3</sup> for both the electrons and holes also show linear Dirac-type bare kinetic-energy dispersion spectra in 2D graphene monolayers due to the honeycomb lattice structure of carbon atoms. The spectacular findings are universal minimum conductivity of the order of quantum conductance  $e^2/h$ , anomalous half integer quantum Hall effect, cyclotron mass  $m_c$  of massless carriers in graphene described by  $E = m_c v_F^2$  ( $v_F$  is the Fermi velocity), and high mobility of samples which is basically independent of doping and temperature.<sup>2,3</sup>

Hwang *et al.*<sup>4</sup> have given a theory for 2D graphene carrier transport, and its quantitative agreement with the existing experimental data strongly indicates that the dominant carrier scattering mechanism is due to charged impurities located near the interface between the graphene and the substrate. In their later work<sup>5</sup> it is shown that adsorbed molecules, acting as compensators that partially neutralize the random charged impurity centers in the substrate, enhance graphene mobility without much change in the carrier density. Microscopic ripples<sup>6</sup> are believed to be another scattering mechanism limiting the mobility. In a phenomenological study momentum relaxation times due to contact potential, charged impurities, and acoustic phonons are given. Moreover, an additional scattering mechanism involving midgap states, arising due to local point defects such as vacancies, cracks, etc., is discussed leading to similar wave vector dependence of its momentum relaxation time as charged impurities to account for the experimental findings.<sup>7</sup>

If all the extrinsic scattering mechanisms such as charged impurities, interface roughness, graphene ripples, etc. can be

eliminated from the system, in principle, then there are intrinsic scatterers such as phonons that cannot be eliminated, and therefore set a fundamental limit on possible intrinsic charge-carrier mobilities and performance of graphene-based devices. Very recent measurements of Morozov *et al.*<sup>8</sup> show that giant intrinsic carrier mobilities higher than  $2 \times 10^5$  cm<sup>2</sup>/V s are achievable if extrinsic disorder is eliminated.

The advantage of graphene over conventional 2D GaAs structures is that polar-optical phonon scattering which dominates at room temperature and the piezoelectric scattering dominating electron-acoustic phonon interaction at low temperature are absent. Hence, a very high room-temperature mobility limited only by acoustic phonon scattering through weak deformation-potential coupling is expected in graphene. Very recently, Hwang and Das Sarma<sup>9</sup> have calculated the intrinsic temperature-dependent 2D graphene mobility limited only by the acoustic phonon scattering, and mobility exceeding  $10^5$  cm<sup>2</sup>/V s is found to be feasible. It is emphasized that in no other system intrinsic room-temperature mobility could reach a value as high as  $10^5$  cm<sup>2</sup>/V s. Due to some uncertainty in the precise quantitative value of deformation-potential coupling constant  $D$ , a quantitative comparison with the experimental data makes it a difficult task.<sup>9</sup> The range of  $D \approx 10-30$  eV is quoted in the literature (see Refs. 7 and 9 and references therein). Unlike the mobility, which depends upon scattering due to lattice disorders and phonons, the low-temperature phonon drag thermopower  $S^g$  and electron energy-loss rate  $P$  depend only on electron-acoustic phonon scattering. Both  $S^g$  and  $P$  are sensitive measures of electron-phonon ( $e-p$ ) coupling, each of which determine  $e-p$  coupling independently.  $S^g$  and  $P$  have been exhaustively studied for a two-dimensional electron gas (2DEG) in Si metal-oxide-semiconductor field-effect transistors (Si-MOSFETs) and GaAs heterojunctions.<sup>10-18</sup> The uncertainty in the value of  $D$  in graphene is similar to the case of 2DEG in GaAs heterojunctions with  $D = 7-16$  eV,<sup>16,17,19</sup> and  $S^g$  and  $P$  studies are used to resolve this issue. The low-temperature study of  $S^g$  and  $P$  in 2D graphene both theoretically and experimentally could help and provide a more reliable estimate of the deformation-potential coupling constant.  $S^g$  is calculated in a one-dimensional system of single walled carbon nanotubes.<sup>20</sup> In

the present work we give the calculations of low temperature  $S^g$  and  $P$  in 2D graphene by considering 2D electron interaction with 2D acoustic phonons via deformation-potential coupling.

## II. THEORY

The low energy-band structure of graphene is modeled as cones, located at two equivalent Brillouin-zone corners, with the linear relation between energy and momentum of the electrons given by  $E_k = \hbar v_F |\mathbf{k}|$ , where  $\mathbf{k} = (k_x, k_y)$  is the 2D electron wave vector and  $v_F$  is the Fermi velocity of graphene which is independent of carrier density. The density of states  $D(E_k) = (g_s g_v / 2\pi \hbar^2) E_k / v_F^2$ , where  $g_s$  is the spin degeneracy and  $g_v$  is the valley degeneracy.

### A. Phonon drag thermopower

An applied temperature gradient  $\nabla T$  causes flow of electrons and phonons from hotter to cooler region. Flow of electrons produces diffusion thermopower  $S^d$ . Flow of phonons carries a momentum current, and a fraction of it is transferred to electrons due to electron-phonon interaction, producing an electron current density  $\mathbf{J}$ . In the open circuit condition an electric field  $\mathbf{E} = S^g \nabla T$  is set up to stop  $\mathbf{J}$ . At low temperatures  $S^g$  dominates over  $S^d$  in a usual 2DEG.<sup>11-13</sup> Cantrell and Butcher<sup>10</sup> have given the standard theory of  $S^g$  of 2D electrons coupled to three-dimensional (3D) phonons. Following Cantrell and Butcher,<sup>10</sup> with appropriate modifications, we develop a theory to calculate  $S^g$  in 2D graphene where 2D electrons interact with 2D acoustic phonons of energy  $\hbar \omega_{\mathbf{q}}$  and wave vector  $\mathbf{q} = (q_x, q_y)$ . It can be shown that  $S^g$  is given by

$$S^g = \frac{2e}{A \sigma k_B T^2} \sum_{\mathbf{k}, \mathbf{k}', \mathbf{q}} \hbar \omega_{\mathbf{q}} f(E_{\mathbf{k}}) \times [(1 - f(E_{\mathbf{k}'})] P_{\mathbf{q}}^a(\mathbf{k}, \mathbf{k}') \tau_p \mathbf{v}_p \cdot (\mathbf{v}_{\mathbf{k}} \tau_{\mathbf{k}} - \mathbf{v}_{\mathbf{k}'} \tau_{\mathbf{k}'}), \quad (1)$$

where the factor of 2 is due to valley degeneracy  $g_v = 2$  (spin degeneracy  $g_s = 2$  is already taken into account in the Cantrell-Butcher formula),  $e$  is the magnitude of the electron charge,  $A$  is the area of the graphene,  $\sigma$  is the electrical conductivity,  $f(E_{\mathbf{k}})$  is the Fermi-Dirac function,  $\omega_{\mathbf{q}} = v_s |\mathbf{q}|$ ,  $\mathbf{v}_p = v_s \mathbf{q} / |\mathbf{q}|$  is the phonon group velocity,  $v_s$  is the sound velocity in graphene,  $\mathbf{v}_{\mathbf{k}} = v_F \mathbf{k} / |\mathbf{k}|$  is the velocity of the electron in state  $\mathbf{k}$ ,  $\tau_{\mathbf{k}}$  is the electron momentum relaxation time, and  $\tau_{\mathbf{q}}$  is the phonon relaxation time. Finally,  $P_{\mathbf{q}}^a(\mathbf{k}, \mathbf{k}')$  is the transition rate at which the electron in state  $\mathbf{k}$  makes the transition to state  $\mathbf{k}'$  by absorbing a phonon, and it is given by

$$P_{\mathbf{q}}^a(\mathbf{k}, \mathbf{k}') = \frac{2\pi}{\hbar} |C(\mathbf{q})|^2 N_{\mathbf{q}} \delta_{\mathbf{k}', \mathbf{k} + \mathbf{q}} \delta(E_{\mathbf{k}} + \hbar \omega_{\mathbf{q}} - E_{\mathbf{k}'}). \quad (2)$$

Here  $|C(\mathbf{q})|^2$  is the electron-acoustic phonon matrix element,  $N_{\mathbf{q}} = [\exp(\hbar \omega_{\mathbf{q}} / k_B T) - 1]^{-1}$  is the phonon distribution function, and  $\mathbf{q} = \mathbf{k}' - \mathbf{k}$ . We assume that  $\tau_{\mathbf{k}}$  is function of only  $E_{\mathbf{k}}$  and varies very slowly over energy range  $\hbar \omega_{\mathbf{q}}$ . Then, using equations for  $\mathbf{v}_p$  and  $\mathbf{v}_{\mathbf{k}}$ , and since  $\hbar \omega_{\mathbf{q}} \ll E_F$  ( $E_F \sim 0.1$  eV), in the quasielastic approximation,<sup>19</sup> we find

$$\begin{aligned} \mathbf{v}_p \cdot (\mathbf{v}_{\mathbf{k}} \tau_{\mathbf{k}} - \mathbf{v}_{\mathbf{k}'} \tau_{\mathbf{k}'}) &= -v_s v_F \tau(E_{\mathbf{k}}) (4k/q) \sin^2(\theta/2) \\ &= -[4v_s v_F \tau(E_{\mathbf{k}}) E_{\mathbf{k}} / (\hbar v_F q)] \sin^2(\theta/2), \end{aligned} \quad (3)$$

where  $\theta$  is the angle between  $\mathbf{k}$  and  $\mathbf{k}'$ . Since  $\mathbf{q} = \mathbf{k}' - \mathbf{k}$ , we can retain the summation over  $\mathbf{k}$  and  $\mathbf{k}'$ . The summation over  $\mathbf{k}'$  is replaced by the integral

$$\sum_{\mathbf{k}'} \rightarrow \frac{A}{4\pi^2} \int_0^\infty k' dk' \int_{-\pi}^\pi d\theta = \frac{A}{4\pi^2 (\hbar v_F)^2} \int_0^\infty dE_{\mathbf{k}'} E_{\mathbf{k}'} \int_{-\pi}^\pi d\theta. \quad (4)$$

Integrating with respect to  $E_{\mathbf{k}'}$ , in the quasielastic approximation, we obtain

$$\begin{aligned} S^g &= -\frac{4e v_s^2}{\pi \sigma k_B T^2 \hbar^2 v_F} \sum_{\mathbf{k}} \int_{-\pi}^\pi d\theta \tau_p \tau(E_{\mathbf{k}}) E_{\mathbf{k}}^2 \sin^2(\theta/2) f(E_{\mathbf{k}}) \\ &\quad \times [1 - f(E_{\mathbf{k}} + \hbar \omega_{\mathbf{q}})] |C(\mathbf{q})|^2 N_{\mathbf{q}}. \end{aligned} \quad (5)$$

Now the summation over  $\mathbf{k}$  is converted to integration over energy, which gives

$$\sum_{\mathbf{k}} \rightarrow \frac{A}{4\pi^2 (\hbar v_F)^2} \int_0^\infty dE_{\mathbf{k}} E_{\mathbf{k}} \int_{-\pi}^\pi d\varphi = \frac{A}{2\pi (\hbar v_F)^2} \int_0^\infty dE_{\mathbf{k}} E_{\mathbf{k}}. \quad (6)$$

The integrand in Eq. (5) is an even function of  $\theta$  and integration with respect to  $\theta$  can be expressed in terms of  $q$  using  $q = 2k |\sin(\theta/2)|$ . Hence, we obtain

$$\begin{aligned} S^g &= -\frac{eA}{\pi^2 \sigma k_B T^2 \hbar^4 v_F} \int_0^\infty dq \int_{\gamma}^\infty dE_{\mathbf{k}} \frac{E_{\mathbf{k}} (\hbar \omega_{\mathbf{q}})^2 \tau_p \tau(E_{\mathbf{k}})}{\sqrt{E_{\mathbf{k}}^2 - \gamma^2}} \\ &\quad \times |C(\mathbf{q})|^2 N_{\mathbf{q}} f(E_{\mathbf{k}}) [1 - f(E_{\mathbf{k}} + \hbar \omega_{\mathbf{q}})]. \end{aligned} \quad (7)$$

The lower limit of integration over  $E_{\mathbf{k}}$  is set to be  $\gamma = \hbar v_F q / 2$ .

The matrix element for deformation-potential scattering is given by<sup>7,9</sup>

$$|C(\mathbf{q})|^2 = \frac{D^2 \hbar q}{2A \rho v_s} \left[ 1 - \left( \frac{q}{2k} \right)^2 \right], \quad (8)$$

where  $\rho$  is the graphene mass density. At low temperatures phonon scattering is assumed to be dominated by boundary scattering and  $\tau_p = \Lambda / v_s$ , where  $\Lambda$  is the phonon mean-free path assumed to be independent of  $\mathbf{q}$ . Moreover,  $\tau(E_{\mathbf{k}})$  is assumed to vary slowly near  $E_{\mathbf{k}} = E_F$ . Then, using  $\sigma = e^2 E_F \tau(E_F) / \pi \hbar^2$ ,<sup>7,9</sup> we obtain

$$\begin{aligned} S^g &= -\frac{D^2 \Lambda}{2\pi \rho e E_F k_B T^2 \hbar^2 v_s^3 v_F} \int_0^\infty dq \int_{\gamma}^\infty dE_{\mathbf{k}} (\hbar \omega_{\mathbf{q}})^3 \sqrt{1 - (\gamma/E_{\mathbf{k}})^2} \\ &\quad \times N_{\mathbf{q}} f(E_{\mathbf{k}}) [1 - f(E_{\mathbf{k}} + \hbar \omega_{\mathbf{q}})]. \end{aligned} \quad (9)$$

At very low temperatures we can make the following approximation:

$$f(E_{\mathbf{k}}) [1 - f(E_{\mathbf{k}} + \hbar \omega_{\mathbf{q}})] \approx \hbar \omega_{\mathbf{q}} (N_{\mathbf{q}} + 1) \delta(E_{\mathbf{k}} - E_F). \quad (10)$$

Then, the  $E_{\mathbf{k}}$  integration gives

$$S^g = -\frac{D^2\Lambda}{2\pi\rho eE_F k_B T^2 \hbar^2 v_s^3 v_F} \int_0^\infty dq (\hbar\omega_q)^4 N_q \times (N_q + 1) \sqrt{1 - (\gamma/E_F)^2} \theta(1 - (\gamma/E_F)). \quad (11)$$

Here,  $\theta(x)=1$  for  $x \geq 0$  and  $\theta(x)=0$  for  $x < 0$ .

In the low-temperature region, the Bloch-Gruneisen (BG) regime  $T \ll T_{BG}$  is defined by a characteristic temperature  $k_B T_{BG} = 2\hbar v_s k_F$ . In graphene  $T_{BG} = 54 \sqrt{n_s}$  K with 2D carrier density  $n_s$  measured in units of  $10^{12} \text{ cm}^{-2}$ . In the BG regime  $\hbar\omega_q \sim k_B T$ . An essential requirement for very low  $T$  behavior is  $q \ll k_F$ . Theoretical findings of phonon limited mobility in graphene show BG power-law behavior of  $T^4$  ( $T^6$ ) for unscreened (screened) deformation-potential coupling.<sup>9</sup> In the ultralow  $T$  region  $q \rightarrow 0$  and  $\sqrt{1 - (\gamma/E_F)^2} \rightarrow 1$ , then we get an approximated equation for  $S^g$  with a simple power law

$$S^g = -\frac{D^2\Lambda k_B^4 T^3 4! \zeta(4)}{2\pi e \rho E_F \hbar^3 v_s^4 v_F}, \quad (12)$$

where  $\zeta(n)$  is the Riemann zeta function.

In order to see the relative contribution of  $S^g$  to the total phonon drag thermopower  $S = S^d + S^g$ , we briefly examine  $S^d$  of the 2DEG in graphene. Using Mott formula  $S^d = -(\pi^2 k_B^2 T / 3e) [d\sigma(E_k) / dE_k]_{E_k=E_F}$ , with  $\tau(E_k) \sim E_k^p$ , we obtain

$$S^d = -\frac{\pi^2 k_B^2 T (p+1)}{3e E_F}. \quad (13)$$

In the phenomenological study of electronic transport coefficients,<sup>7</sup> this equation is obtained for screened Coulomb potential scattering with  $p=1$ .

### B. Energy-loss rate

The acoustic phonon emission process governs the thermal relaxation of hot electrons at low temperatures. This has been extensively studied both experimentally and theoretically for a 2DEG in GaAs heterojunctions and Si-MOSFET.<sup>14–18</sup> In graphene-related materials, the energies of optical phonons are of the order of 0.1–0.2 eV and hot-electron energy relaxation is considered to be only due to acoustic phonons even at room temperature. To calculate energy-loss rate  $P$  the “electron temperature model” in which electrons are assumed to have Fermi-Dirac distribution  $f(E_k)$  with an electron temperature  $T_e$  greater than the lattice temperature  $T$ . The average energy-loss rate via acoustic phonon emission is given by<sup>16,21</sup>

$$P = -\frac{1}{N_e} \sum_{\mathbf{q}} \hbar\omega_{\mathbf{q}} \frac{dN_{\mathbf{q}}}{dt}, \quad (14)$$

where  $N_e$  is the total number of electrons and the rate of change in phonon distribution

$$\frac{dN_{\mathbf{q}}}{dt} = 4 \left( \frac{2\pi}{\hbar} \right) \sum_{\mathbf{k}} |C(\mathbf{q})|^2 \delta(E_{\mathbf{k}} + \hbar\omega_{\mathbf{q}} - E_{\mathbf{k}'}) \delta_{\mathbf{k}', \mathbf{k}+\mathbf{q}} \times \{ (N_{\mathbf{q}} + 1) f(E_{\mathbf{k}'}) [1 - f(E_{\mathbf{k}})] - N_{\mathbf{q}} f(E_{\mathbf{k}}) [1 - f(E_{\mathbf{k}'})] \}. \quad (15)$$

The factor of 4 in the above equation is to account for spin and valley degeneracies. To calculate  $P$ , we follow the same steps as in the evaluation of  $S^g$  and obtain

$$P = F(T_e) - F(T), \quad (16)$$

where

$$F(T) = -\frac{D^2}{n_s \rho \pi^2 \hbar^4 v_s^2 v_F^3} \int_0^\infty dq \int_{\gamma}^\infty dE_{\mathbf{k}} (\hbar\omega_{\mathbf{q}})^2 \sqrt{E_{\mathbf{k}}^2 - \gamma^2} N_{\mathbf{q}}(T) \times [f(E_{\mathbf{k}}) - f(E_{\mathbf{k}} + \hbar\omega_{\mathbf{q}})]. \quad (17)$$

At low temperatures, we approximate

$$f(E_{\mathbf{k}}) - f(E_{\mathbf{k}} + \hbar\omega_{\mathbf{q}}) \approx \hbar\omega_{\mathbf{q}} \delta(E_{\mathbf{k}} - E_F). \quad (18)$$

Then, we obtain

$$F(T) = -\frac{D^2 E_F}{n_s \rho \pi^2 \hbar^4 v_s^2 v_F^3} \int_0^\infty dq (\hbar\omega_{\mathbf{q}})^3 \sqrt{1 - (\gamma/E_F)^2} N_{\mathbf{q}}(T) \times \theta(1 - (\gamma/E_F)). \quad (19)$$

In the limit of  $q \rightarrow 0$ , we get an approximated equation in the form of power law

$$F(T) = -\frac{D^2 E_F (k_B T)^4 3! \zeta(4)}{n_s \pi^2 \rho \hbar^5 v_s^3 v_F^3}. \quad (20)$$

The expressions for  $S^g$  and  $F(T)$  are obtained based on the same basic assumptions with the same  $e$ - $p$  interaction, and their very low  $T$  approximated Eqs. (13) and (21) have many common factors. One can obtain a simple relation between  $S^g$  and  $F(T)$

$$F(T) = \xi S^g v_s e T / \Lambda, \quad (21)$$

where  $\xi$  is the numerical constant of the order of unity. At very low  $T$ ,  $\xi=0.5$ . This relation provides a very useful way of predicting either one of  $S^g$  or  $F(T)$ , with the other given for the 2DEG in graphene as done in Si-MOSFET.<sup>14</sup>

## III. RESULTS AND DISCUSSION

We numerically evaluate  $S^g$  and  $P$  using the 2D graphene parameters:<sup>9</sup>  $\rho = 7.6 \times 10^{-8} \text{ g/cm}^{-2}$ ,  $v_F = 9.874 \times 10^7 \text{ cm/s}$ ,  $D = 19 \text{ eV}$ , and  $v_s = 2 \times 10^6 \text{ cm/s}$ .  $S^g$  and  $P$  are studied as a function of temperature and electron concentration. The effects of screening can be taken into account by dividing the matrix element by the dielectric function.<sup>22</sup> However, screening effects are ignored as the matrix elements in graphene arise from the change in the overlap between orbitals placed on different atoms and not from a Coulomb potential.<sup>9</sup>

### A. Phonon drag thermopower

$S^g$  is studied as a function of  $T$  in the range of 0.5–10 K for the range of  $n_s = (1-10) \times 10^{12} \text{ cm}^{-2}$  with  $\Lambda = 10 \text{ nm}$ .<sup>20</sup>

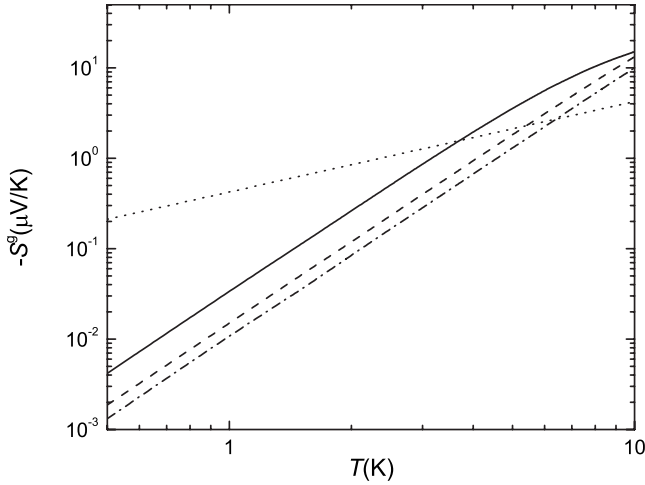


FIG. 1. Phonon drag thermopower  $S^g$  versus temperature  $T$  for  $n_s=1.0 \times 10^{12} \text{ cm}^{-2}$  (solid curve),  $n_s=5.0 \times 10^{12} \text{ cm}^{-2}$  (dashed curve), and  $n_s=10.0 \times 10^{12} \text{ cm}^{-2}$  (dot-dashed curve). Dotted curve is diffusion thermopower  $S^d$ , with  $p=1$ , for  $n_s=1.0 \times 10^{12} \text{ cm}^{-2}$ .

$S^g$  calculated using Eq. (9) as a function of  $T$  is shown in Fig. 1 by solid, dashed, and dot-dashed curves, respectively, for  $n_s=1.0 \times 10^{12}$ ,  $5.0 \times 10^{12}$ , and  $10 \times 10^{12} \text{ cm}^{-2}$ . The nature of the curves is similar to that of a usual 2DEG.  $S^g$  is expected to flatten for larger temperatures as  $\tau_p$  is assumed to be independent of temperature. For larger temperatures, it is possible that phonon-phonon scattering may become important, introducing temperature dependence of  $\tau_p$ .<sup>20</sup>

In the limit of  $q \rightarrow 0$ , i.e., for very small  $T$ , approximated Eq. (12) gives  $S^g \sim T^3$  dependence in contrast to the  $S^g \sim T^4$  dependence of unscreened deformation-potential scattering in the usual 2DEG. The 2D nature of acoustic phonons reduces power of  $T$  by unity from its 3D value. From our calculation we observed that at higher temperatures Eq. (9) gives  $S^g$  values which are smaller than the values obtained from the power law [Eq. (12)]. Simple power-law dependence is obeyed up to  $T=5.0 \text{ K}$  for  $n_s=1.0 \times 10^{12} \text{ cm}^{-2}$  and up to  $T=10.0 \text{ K}$  for  $n_s=10.0 \times 10^{12} \text{ cm}^{-2}$ . We attribute this to the function  $\sqrt{1-(\gamma/E_F)^2}$  in Eq. (9) which reduces  $S^g$ . For example, at  $T=10 \text{ K}$   $S^g$  is reduced nearly by a factor of 2 for  $n_s=1.0 \times 10^{12} \text{ cm}^{-2}$ .

In the low-temperature limit,  $S^g$  and phonon limited mobility  $\mu_p$  are related by Herring's formula  $S^g \mu_p \sim T^{-1}$  in bulk semiconductors,<sup>23</sup> Si-MOSFET, and GaAs heterojunction.<sup>11-13,24</sup> In 2D graphene  $\mu_p \sim T^{-4}$  (Ref. 9) and  $S^g \sim T^3$ . Then we obtain  $S^g \mu_p \sim T^{-1}$  which validates Herring's law in 2D graphene in which 2D electrons with linear dispersion interact with 2D phonons with  $\omega_q \sim q$ . In fact, using the momentum relaxation time in the low-temperature limit [Eq. (11) of Ref. 9], we obtain  $S^g \mu_p = -v_s \Lambda T^{-1}$ , a simple and straightforward relation, which is the same as in 3D semiconductors and 2D systems for one acoustic branch. Consequently and interestingly, in the low-temperature limit,  $S^g$  is used to provide the most accurate way of measuring  $\mu_p$  in the 2D GaAs system even at half filling factor in the fractional quantum Hall regime.<sup>25</sup> However, it is to be noted that, in a semiconductor thin film for 2D phonons with  $\omega_q$

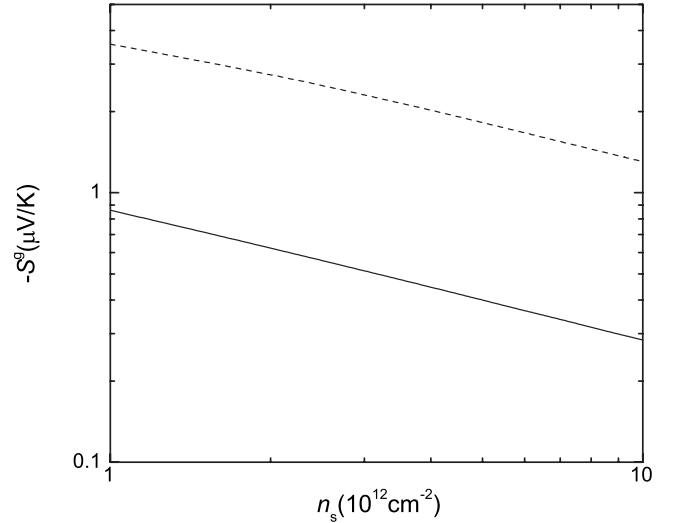


FIG. 2. Phonon drag thermopower  $S^g$  versus electron concentration  $n_s$  for  $T=3.0 \text{ K}$  (solid curve) and  $T=5.0 \text{ K}$  (dashed curve).

$\sim q^2$  (flexural modes), Herring's law is invalidated where, as for phonons with  $\omega_q \sim q$  (dilatational modes), it is found to be valid.<sup>26</sup> It indicates that the nonlinear dispersion of phonons with their group velocity being  $\mathbf{q}$  dependent may lead to invalidation of Herring's law irrespective of electron dispersion.

We also show  $S^d$  versus  $T$  (dotted curve in Fig. 1) obtained from Eq. (13) with  $p=1$ . This curve is for  $n_s=1.0 \times 10^{12} \text{ cm}^{-2}$ . Scattering due to ionized impurities and vacancies give  $p=1$ .<sup>7</sup> The relative magnitudes of  $S^g$  and  $S^d$  depend upon phonon mean-free path  $\Lambda$ ,  $n_s$ ,  $T$ , and  $p$ . With the choice of parameters in the present calculation,  $S^d$  is dominant in the low-temperature region. It is interesting to note that  $S^d$  will be zero if  $p=-1$ . The scattering due to the contact potential gives  $p=-1$ .<sup>7</sup> If scattering due to ionized impurities, ripples, and vacancies is eliminated, then  $S^d$  can be made zero. Such a system will be ideal for the study of  $S^g$  in the estimating deformation-potential coupling constant.

From the simple approach of the force balance argument,<sup>11</sup> it is shown that  $S^g \propto f C_v / n_s e$ , where  $C_v$  is the lattice specific and  $f$  is the fraction of momentum lost by the phonons to the carriers. If  $f$  is weakly temperature dependent, then  $S^g$  dependence on  $T$  comes only from  $C_v$ . At very low temperatures, it can be easily shown that  $C_v \sim T^2$  for 2D phonons in graphene giving approximate  $S^g \sim T^2$  dependence. For 3D phonons it gives  $S^g \sim T^3$ , giving a reasonable qualitative agreement with the experimental data in GaAs heterojunctions and Si-MOSFET at liquid-helium temperatures.<sup>11,13</sup>

Since it is feasible to control the carrier density in the graphene plane experimentally,<sup>1</sup> it is possible to check experimentally the  $n_s$  dependence of  $S^g$ . In Fig. 2, we show  $S^g$  versus  $n_s$  in the range  $n_s=(1-10) \times 10^{12} \text{ cm}^{-2}$  at  $T=3.0$  (solid curve) and  $5.0 \text{ K}$  (dashed curve).  $S^g$  shows a weak dependence on  $n_s$  and it is decreasing with the increasing  $n_s$ . For example, at  $5.0 \text{ K}$ , when  $n_s$  is varied from  $1 \times 10^{12}$  to  $10 \times 10^{12} \text{ cm}^{-2}$ ,  $S^g$  reduces by about three times. In the low-temperature limit  $S^g \sim n_s^{-1/2}$  in graphene whereas  $S^g \sim n_s^{-3/2}$  in the usual 2DEG for both screened and unscreened cases.

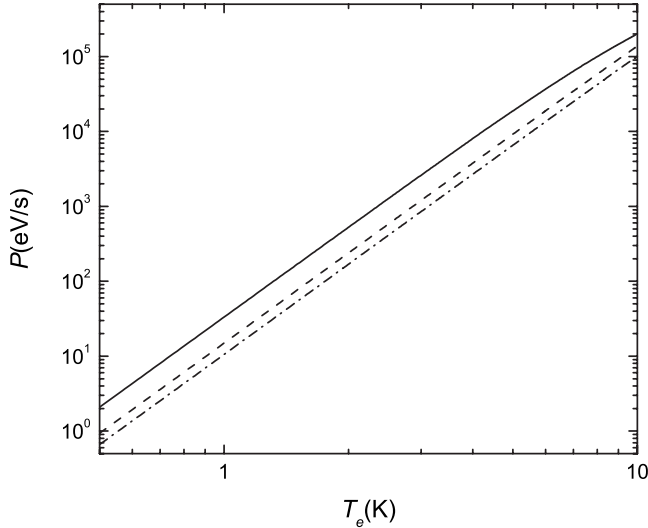


FIG. 3. Electron energy-loss rate  $P$  versus electron temperature  $T_e$ , at lattice temperature  $T=0$  K, for  $n_s=1.0 \times 10^{12}$  cm $^{-2}$  (solid curve),  $n_s=5.0 \times 10^{12}$  cm $^{-2}$  (dashed curve), and  $n_s=10.0 \times 10^{12}$  cm $^{-2}$  (dot-dashed curve).

$S^d \sim n_s^{-1/2}$  in graphene and  $\sim n_s^{-1}$  in the case of the usual 2DEG.

### B. Energy-loss rate

Figure 3 shows energy-loss rate  $P=F(T_e)$  per electron as a function of electron temperature  $T_e$  in the range of 0.5–10 K for  $n_s=1.0 \times 10^{12}$  (solid curve),  $5.0 \times 10^{12}$  (dashed curve), and  $10.0 \times 10^{12}$  cm $^{-2}$  (dot-dashed curve) at lattice temperature  $T=0$ . Results are due to Eq. (17). We observe that, as in the case of  $S^g$ , approximated Eq. (20) overestimates  $F(T_e)$  in the higher temperature region which is again ascribed to  $\sqrt{1-(\gamma/E_F)^2}$ . Approximated Eq. (20) gives a simple power law of  $F(T) \sim T^4$  contrary to  $F(T) \sim T^5$  due to unscreened deformation-potential coupling in usual 2DEG (Refs. 14, 15, and 17) and for 2DEG in a thin semiconductor film.<sup>27</sup> It is to be noted that power law  $F(T) \sim T^5$  in the semiconductor thin film is for 2D dilatational modes with  $\omega_q \sim q$  and is obtained from the energy relaxation time  $\tau_e$  calculation of Ref. 27 using the relation  $\tau_e^{-1} \sim (1/C_e)(dP/dT_e)$ ,<sup>28</sup> where  $C_e$  is the electronic specific heat. Since  $C_e \sim D(E_F)$ , in graphene, it will lead to different  $n_s$  dependence for  $\tau_e^{-1}$  and  $F(T_e)$  unlike the usual 2DEG where  $D(E_F)$  is independent of  $n_s$ . We would like to point out that low-temperature studies of  $F(T)$  in graphene will avoid a possible additional “intervalley” phonon scattering which becomes significant at high temperatures.<sup>9</sup>

In Fig. 4,  $P$  is shown as a function of  $n_s$  for  $n_s=(1-10) \times 10^{12}$  cm $^{-2}$  at  $T_e=3.0$  (solid curve) and 5.0 K (dashed curve) for  $T=0$  K. Again  $F(T)$  has a weak dependence on  $n_s$ . In the very low-temperature limit  $F(T) \sim n_s^{-1/2}$ , which is the same as for  $S^g$ , whereas,  $F(T) \sim n_s^{-3/2}$  for deformation-potential coupling in the usual 2DEG,<sup>14</sup> and for the 2DEG in semiconductor thin films<sup>27</sup> for both screened and unscreened interactions.

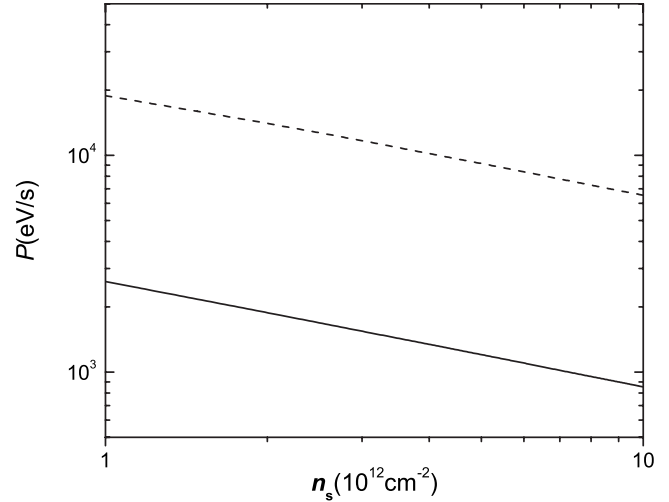


FIG. 4. Electron energy-loss rate  $P$  versus electron concentration  $n_s$  for  $T_e=3.0$  K (solid curve) and  $T_e=5.0$  K (dashed curve) with  $T=0$  K.

We would like to make some more comparisons of  $S^g$  and  $F(T)$  in graphene with those in Si-MOSFET (Ref. 14) although an exact comparison may not be possible due to massless electron in graphene.  $S^g$  and  $F(T) \sim D^2$ , and  $S^g \sim \Lambda$  as in Si-MOSFET. Any change in the value of  $D$  changes the values of  $S^g$  and  $F(T)$  by its square. In MOSFET  $\Lambda \sim 0.5$  mm whereas  $\Lambda \sim 10$   $\mu$ m chosen in our calculation is about an order of magnitude smaller. In graphene  $\Lambda$  may vary in the range of 1–100  $\mu$ m. Besides, in the low-temperature limit we see that  $S^g \sim v_s^{-4}$  and  $F(T) \sim v_s^{-3}$  in graphene, and  $S^g \sim v_s^{-5}$  and  $F(T) \sim v_s^{-4}$  for unscreened deformation-potential coupling in Si-MOSFET.<sup>14</sup> In Si-MOSFET  $v_s=v_l=5.269 \times 10^5$  cm/s for transverse-acoustic (TA) phonons and  $v_s=v_l=8.834 \times 10^5$  cm/s for longitudinal-acoustic (LA) phonons which are smaller by a factor of about four and two, respectively, compared to the value of  $v_s=2.0 \times 10^6$  cm/s in graphene used in our calculation. In Si-MOSFET  $S^g$  and  $F(T)$  due to TA phonons give a major contribution because of the smaller value of  $v_l$ . Four times larger value of  $v_s$  in graphene may make the values of  $S^g$  and  $F(T)$  about 100 times smaller than their respective values in Si-MOSFET for the unscreened case. A similar comparison may be made with  $S^g$  and  $F(T)$  due to unscreened deformation-potential coupling in GaAs heterojunctions.<sup>13,15,17</sup>

We would like to point out that in graphene different values of  $v_s$  are being used in the literature. For example,  $v_s=2.0 \times 10^6$  cm/s (Refs. 9 and 20) and  $v_l=2.82 \times 10^5$  cm/s for TA phonons,<sup>7</sup> and  $v_l=7.33 \times 10^5$  cm/s for LA phonons.<sup>7,29</sup> For  $v_l=7.33 \times 10^5$  cm/s,  $S^g$  and  $F(T)$  will be enhanced by about one to two orders of magnitude.

As discussed in Ref. 9, dividing the  $e$ - $p$  interaction matrix element by the dielectric function,<sup>22</sup> in the low-temperature limit, gives  $S^g \sim T^5$ ,  $F(T) \sim T^4$ ,  $S^g, F(T) \sim n_s^{-3/2}$ ,  $S^g \sim v_s^{-6}$ , and  $F(T) \sim v_s^{-5}$ .  $S^g$  and  $F(T)$  values will be reduced by a few orders of magnitude as in Si-MOSFET and GaAs heterojunction.

It is worth noting that, due to electron-hole symmetry (i.e., with the Fermi energy or chemical potential  $\mu=0$ ), ther-

mopower vanishes in single wall carbon nanotubes<sup>30,31</sup> and graphene.<sup>32</sup> However, large thermopower can be obtained by breaking the electron-hole symmetry. Defect states do break symmetry and may lead to large value of the thermopower.<sup>31,32</sup> In our calculation the contribution due only to electrons is considered which may overestimate  $S^g$ .

#### IV. CONCLUSIONS

Using the unscreened acoustic deformation-potential coupling, the phonon drag thermopower  $S^g$  and hot-electron energy-loss rate  $F(T)$  are theoretically studied in 2D graphene at low temperatures. Since  $S^g$  and  $F(T)$  are sensitive measures of electron acoustic phonon coupling, their theoretical and experimental studies may help in removing the existing ambiguity in the value of deformation-potential

constant  $D$  in graphene. Although we have used  $D=19$  eV (Ref. 9) in all our numerical calculations for illustration, one can change  $D$  by scaling our results by  $D^2$ . Large values of  $v_F$  and  $v_s$  in graphene may lead to the smaller values of  $S^g$  and  $F(T)$  compared to their respective values in usual 2D systems. In the low-temperature limit we find  $S^g \sim T^3$  and  $F(T) \sim T^4$ , and  $S^g$  and  $F(T) \sim n_s^{-1/2}$ . Herring's law is also validated in graphene in which electron and phonon dispersions are linear. Our calculations may require extensions and modifications at high temperatures to include inelasticity of electron scattering and phonon scattering by impurities and phonons in the study of  $S^g$ , and intervalley phonon scattering in the study of  $F(T)$ . These properties remain to be investigated experimentally to compare with the theory developed in the present work. Measurements of  $S^g$  require separation of  $S^d$  from measured  $S$ .

- 
- <sup>1</sup>K. S. Novoselov, A. K. Geim, S. V. Morozov, D. Jiang, Y. Zhang, S. V. Dubonos, I. V. Grigorieva, and A. A. Firsov, *Science* **306**, 666 (2004).
- <sup>2</sup>K. S. Novoselov, A. K. Geim, S. V. Morozov, D. Jiang, M. I. Katsnelson, I. V. Grigorieva, S. V. Dubonos, and A. A. Firsov, *Nature (London)* **438**, 197 (2005).
- <sup>3</sup>Y. Zhang, Y. Jan, H. L. Stormer, and P. Kim, *Nature (London)* **438**, 201 (2005).
- <sup>4</sup>E. H. Hwang, S. Adam, and S. Das Sarma, *Phys. Rev. Lett.* **98**, 186806 (2007).
- <sup>5</sup>E. H. Hwang, S. Adam, and S. Das Sarma, *Phys. Rev. B* **76**, 195421 (2007).
- <sup>6</sup>F. Schedin, A. K. Geim, S. V. Morozov, D. Jiang, E. H. Hill, P. Blake, and K. S. Novoselov, *Nature Mater.* **6**, 652 (2007); M. I. Katsnelson and A. K. Geim, *Philos. Trans. R. Soc. London, Ser. A* **366**, 195 (2008).
- <sup>7</sup>T. Stauber, N. M. R. Peres, and F. Guinea, *Phys. Rev. B* **76**, 205423 (2007); N. M. R. Peres, J. M. B. Lopes dos Santos, and T. Stauber, *ibid.* **76**, 073412 (2007).
- <sup>8</sup>S. V. Morozov, K. S. Novoselov, M. I. Katsnelson, F. Schedin, D. Elias, J. A. Jaszczak, and A. K. Geim, *Phys. Rev. Lett.* **100**, 016602 (2008).
- <sup>9</sup>E. H. Hwang and S. Das Sarma, *Phys. Rev. B* **77**, 115449 (2008).
- <sup>10</sup>D. G. Cantrell and P. N. Butcher, *J. Phys. C* **20**, 1985 (1987); **20**, 1993 (1987).
- <sup>11</sup>B. L. Gallagher and P. N. Butcher, in *Handbook on Semiconductors*, edited by P. T. Landsberg (Elsevier, Amsterdam, 1992), Vol. 1, p. 817.
- <sup>12</sup>R. Fletcher, *Semicond. Sci. Technol.* **14**, R1 (1999).
- <sup>13</sup>R. Fletcher, E. Zaremba, and U. Zeitler, in *Electron-Phonon Interactions in Low Dimensional Structures*, edited by L. Challis (Oxford Science, Oxford, 2003), p. 149.
- <sup>14</sup>R. Fletcher, V. M. Pudalov, Y. Feng, M. Tsaousidou, and P. N. Butcher, *Phys. Rev. B* **56**, 12422 (1997).
- <sup>15</sup>P. J. Price, *J. Appl. Phys.* **53**, 6863 (1982).
- <sup>16</sup>S. J. Manion, M. Artaki, M. A. Emanuel, J. J. Coleman, and K. Hess, *Phys. Rev. B* **35**, 9203 (1987); Y. Okuyama and N. Tokuda, *ibid.* **40**, 9744 (1989); T. Kawamura, S. Das Sarma, R. Jalabert, and J. K. Jain, *ibid.* **42**, 5407 (1990).
- <sup>17</sup>Y. Ma, R. Fletcher, E. Zaremba, M. DiIorio, C. T. Foxon, and J. J. Harris, *Phys. Rev. B* **43**, 9033 (1991).
- <sup>18</sup>D. V. Khveshchenko and M. Reizer, *Phys. Rev. B* **56**, 15822 (1997); R. Fletcher, Y. Feng, C. T. Foxon, and J. J. Harris, *ibid.* **61**, 2028 (2000).
- <sup>19</sup>H. L. Stormer, L. N. Pfeiffer, K. W. Baldwin, and K. W. West, *Phys. Rev. B* **41**, 1278 (1990); T. Kawamura and S. Das Sarma, *ibid.* **45**, 3612 (1992).
- <sup>20</sup>V. W. Scarola and G. D. Mahan, *Phys. Rev. B* **66**, 205405 (2002).
- <sup>21</sup>E. M. Conwell, *Solid State Physics Supplement* (Academic, New York, 1967), Vol. 9, p. 119.
- <sup>22</sup>E. H. Hwang and S. Das Sarma, *Phys. Rev. B* **75**, 205418 (2007).
- <sup>23</sup>C. Herring, *Phys. Rev.* **96**, 1163 (1954).
- <sup>24</sup>M. Tsaousidou, P. N. Butcher, and G. P. Triberis, *Phys. Rev. B* **64**, 165304 (2001).
- <sup>25</sup>B. Tieke, R. Fletcher, U. Zeitler, M. Henini, and J. C. Maan, *Phys. Rev. B* **58**, 2017 (1998).
- <sup>26</sup>S. S. Kubakaddi, *Phys. Rev. B* **69**, 035317 (2004).
- <sup>27</sup>B. A. Glavin, V. I. Pipa, V. V. Mitin, and M. A. Stroschio, *Phys. Rev. B* **65**, 205315 (2002).
- <sup>28</sup>Edmand Chow, H. P. Wei, S. M. Girvin, and M. Shayegan, *Phys. Rev. Lett.* **77**, 1143 (1996).
- <sup>29</sup>F. T. Vasko and V. Ryzhii, *Phys. Rev. B* **76**, 233404 (2007).
- <sup>30</sup>M. A. Kuroda and J. P. Leburton, arXiv:0807.4756 (unpublished).
- <sup>31</sup>G. D. Mahan, *Phys. Rev. B* **69**, 125407 (2004).
- <sup>32</sup>B. Dora and P. Thalmeier, *Phys. Rev. B* **76**, 035402 (2007); T. Lofwander and M. Fogelstrom, *ibid.* **76**, 193401 (2007).